https://doi.org/10.5194/bg-2019-483
Preprint. Discussion started: 28 January 2020

Biogeosciences Discussions

A revised northern soil Hg pool, based on western Siberia permafrost peat Hg and carbon observations

Artem G. LIM[1], MARTIN JISKRA[2], Jeroen E. SONKE[3],

Sergey V. LOIKO[1], NATALIA KOSYKH[4], Oleg S. POKROVSKY[3,5*]

[1] *BIO-GEO-CLIM Laboratory, Tomsk State University, Tomsk, Russia*
[2] *University of Basel, Environmental Geosciences, Bernoullistrasse 30, 4056 Basel, Switzerland*
[3] *Geosciences and Environment Toulouse, UMR 5563 CNRS, 14 Avenue Edouard Belin 31400 Toulouse, France*
[4] *Lab Biogeocenol, Inst Soil Science & Agrochem, Russian Acad Sci, Siberian Branch, Novosibirsk, Russia*
[5] *N. Laverov Federal Center for Integrated Arctic Research, Russian Academy of Sciences, Arkhangelsk, Russia*

**Email: oleg.pokrovsky@get.omp.eu*

Key words: mercury, peat soil, landscape, bog, , forest, thaw, Siberia

Submitted to *Biogeosciences December 2019*

https://doi.org/10.5194/bg-2019-483
Preprint. Discussion started: 28 January 2020

Biogeosciences Discussions

Abstract

Natural and anthropogenic mercury (Hg) emissions are sequestered in terrestrial soils over short, annual, to long, millennial time scales, before Hg mobilization and run-off impacts wetland and coastal Ocean ecosystems. Recent studies have used Hg to carbon (C) ratios, R_{HgC}, measured in Alaskan permafrost mineral and peat soils, together with a northern soil carbon inventory, to estimate that these soils contain large amounts, 184 to 755 Gg of Hg in the upper 1 m. However, measurements of R_{HgC} on Siberian permafrost peatlands are largely missing, leaving the size of estimated northern soil Hg budget, and its fate under arctic warming scenarios uncertain. Here we present Hg and carbon data for 6 peat cores, down to mineral horizons at 1.5 - 4 m depth, across a 1700 km latitudinal (56 to 67°N) permafrost gradient in the Western Siberian lowlands (WSL). Hg concentrations increase from south to north in all soil horizons, reflecting enhanced net accumulation of atmospheric gaseous Hg by the vegetation Hg pump. The R_{HgC} in WSL peat horizons decreases with depth from 0.38 Gg Pg^{-1} in the active layer to 0.23 Gg Pg^{-1} in continuously frozen peat of the WSL. We estimate the Hg pool (0-1 m) in the permafrost-affected part of WSL peatlands to be 9.3 ± 2.7 Gg. We review and estimate pan-arctic organic and mineral soil R_{HgC} to be 0.19 and 0.77 Gg Pg^{-1}, and use a soil carbon budget to revise the northern soil Hg pool to be 67 Gg (37-88 Gg, interquartile range (IQR)) in the upper 30 cm, 225 Gg (102-320 Gg) in the upper 1 m, and 557 Gg (371-699 Gg) in the upper 3 m. Using the same R_{HgC} approach, we revise the global upper 30 cm soil Hg pool to contain 1078 Gg of Hg (842-1254 Gg, IQR), of which 6% (67 Gg) resides in northern permafrost soils. Additional soil and river studies must be performed in Eastern and Northern Siberia to lower the uncertainty on these estimates, and assess the timing of Hg release to atmosphere and rivers.

https://doi.org/10.5194/bg-2019-483
Preprint. Discussion started: 28 January 2020

1. Introduction

High-latitude organic-rich soils are key ecosystems controlling the transfer of carbon, nutrients, and pollutants between the atmosphere, rivers, lakes and the Arctic Ocean. These soils are most vulnerable to on-going climate change, due to the high mobility of carbon stored in the form of peat deposits. Part of the peat layers are currently frozen but may be subjected to fast thaw, especially in discontinuous and sporadic permafrost zones (Romanovsky et al., 2010). Whilst the stock of C in Arctic and subarctic peat and mineral soils is fairly well quantified (472 Pg C (±27 Pg, 95% confidence interval, CI) in the upper 0-1m (Hugelius et al. 2014), this is not true for pollutants such as mercury (Hg). Because of its strong bio-amplification in Arctic marine biota (Morel et al., 1998), and exposure to native Arctic populations (AMAP, 2011), there is a strong interest in understanding Hg biogeochemistry in Arctic environments (Outridge et al., 2008; Steffen et al., 2008; Stern et al., 2012).

Recent advances in quantifying Arctic Hg cycling show that Arctic Hg^{II} wet deposition is generally low (Pearson et al., 2019), and that the vegetation Hg pump drives yearlong net gaseous Hg^0 (and CO_2) deposition, via foliar uptake to Arctic vegetation and litterfall to soils (Obrist et al. 2017; Jiskra et al. 2018; Jiskra et al., 2019). Soil core analyses in Alaska indicate that large amounts of carbon and Hg have accumulated since the last glacial maximum, and two upscaling approaches to Hg stocks in pan-Arctic permafrost soils resulted in differing estimates of 184 Gg and 755 Gg for the upper 1 m (Schuster et al., 2018; Olson et al., 2018). Despite the overall net atmospheric Hg deposition to soils, research has found that Arctic rivers export 44 Mg y^{-1} of soil Hg, bound to particulate and dissolved organic matter, to the Arctic Ocean (Fisher et al., 2012; Dastoor et al., 2014; Zhang et al., 2015; Sonke et al., 2018). Together with coastal erosion of soils (30 Mg y^{-1}), river Hg inputs constitute a terrestrial Hg flux of 74 Mg y^{-1} to the Arctic Ocean that is of similar magnitude to gross atmospheric deposition over the Arctic Ocean (80 Mg y^{-1}, Sonke et al., 2018). Permafrost thawing has been shown to enhance river Hg export from soils to rivers

https://doi.org/10.5194/bg-2019-483
Preprint. Discussion started: 28 January 2020

(St Pierre et al., 2018), is most pronounced in the discontinuous permafrost zone, and has been suggested to potentially double over the next 50 years (Lim et al., 2019). The quantity of atmospheric Hg deposition to northern peat soils that is presently re-emitted to the atmosphere is not well understood. Hg exchange studies indicate temporally limited Hg^0 emission from the Alaskan permafrost tundra at 68ºN (Obrist et al., 2017), and strong year round net Hg^0 emission from Scandinavian peat at 64ºN (Osterwalder et al., 2018). Other studies provide evidence for vegetation type (Rydberg et al., 2010) and temperature and insolation control (Fahnestock et al., 2019) on net Hg^0 deposition or emission.

All available data of Hg in permafrost soils originate from N-America or Scandinavia (Jensen et al., 1991; Bailey et al., 2002; Talbot et al., 2017; Schuster et al., 2018; Olson et al., 2018). Except for two studies of Hg in a peat profile from a permafrost-free zone of western Siberia (Golovatskaya et al., 2009; Lyapina et al., 2009), we did not find extensive measurements of Hg in peat profiles from permafrost regions of the Russian Arctic and Siberia. Recent work used a soil carbon GIS model to estimate the size of the northern permafrost soil Hg inventory to be 755 ±427 Gg (95% CI) in the upper 1 m (Schuster et al., 2018). However, this estimate is based on extrapolation of high Hg to organic carbon (C) ratios, R_{HgC}, of 1.6 Gg Hg per Pg of C (Gg Pg^{-1}) in Alaskan mineral soils to the entire N-American and Eurasian permafrost zone. A second study used lower R_{HgC}, of 0.12 to 0.62 Gg Pg^{-1}, derived from observations on both Alaskan organic and mineral soils and literature data, to estimate a lower northern soil 0-1 m Hg inventory of 184 Gg (136-274 Gg, 37.5-62.5 percentiles) (Olson et al., 2018). Direct measurement of soil Hg and carbon profiles in frozen peatlands of Siberia are needed to address these variable estimates, and compare the size of permafrost soil Hg pool to the global soil Hg pool. This constitutes the first and main objective of the present study. The second objective was assessing the impact of permafrost type (absent, sporadic, discontinuous and continuous) on Hg concentrations and pools in the active layer, frozen peat and mineral horizons. The third objective

https://doi.org/10.5194/bg-2019-483
Preprint. Discussion started: 28 January 2020

was to relate Hg concentration in peat to that of other trace metals in order to reveal possible mechanisms of Hg and other metal pollutant accumulation within the organic and mineral horizons of frozen peatlands.

2. Study Site and Methods

2.1.Sampling sites

Soil sampling was performed along a latitudinal transect of the western Siberia lowlands (WSL) that comprised the southern taiga (Plotnikovo, 56°N), the middle taiga (Mukhrino, 60°N), the northern part of the taiga zone (Kogalym, 62°N), forest-tundra (Khanymey 62°N and Pangody, 65°N) and tundra (Tazovsky, 67°N) biomes (**Fig. 1**). In the WSL, the permafrost zones follow the temperature and vegetation distribution over the latitude at otherwise similar relief, lithology and runoff, thus allowing to test the effect of permafrost by analyzing latitudinal features of Hg distribution in soils. Key physico-geographical parameters of studied sites and soil types are listed in **Table S1** of the Supplementary Information. The WSL peat actively formed since the beginning of the Holocene until freezing of bogs in the sub-Boreal period (11-4.5 ky, Kremenetski et al., 2003; Panova et al., 2010; Ponomareva et al., 2012; Loiko et al., 2019). Since 4.5 ky, the rate of peat formation and bog extension in the permafrost-affected part of the WSL have decreased. In the southern part of cryolithozone and permafrost-free part of WSL, peat accumulation and bog extension remained active over the entire Holocene (Kurina and Veretennikova, 2015; Preis and Karpenko, 2015; Kurina et al., 2018). The main mineral substrates underlying frozen peat layers of the WSL are quaternary clays, sands, and alevrolites. In the southern part (sites Plotnikovo and Mukhrino), the typical substrate is carbonate-bearing clays of lake-alluvium origin with rare layers of sandstones (**Table S1**).

Mean annual atmospheric temperature (MAAT) increases from south to north, being equal to –0.4, –1.2, –4.0, –5.6, –6.4, and –9.1°C at Plotnikovo, Mukhrino, Kogalym, Khanymey,

https://doi.org/10.5194/bg-2019-483
Preprint. Discussion started: 28 January 2020

Biogeosciences Discussions

Pandogy and Tazovsky, respectively (Trofimova and Balybina, 2014). The permafrost is absent in Plotnikovo but present at all other sites and ranges from relict to isolated (Mukhrino), isolated to sporadic (Kogalym) in the south, to discontinuous (Khanymey, Pangody) and continuous (Tazovsky) in the north. At permafrost-affected sites, the average active (unfrozen) layer thickness (ALT) at the time of sampling of peat mounds (hummocks) ranged from 90 cm in the south to 45 cm in the north. The peat mounds of ombrotrophic bogs probed in this work are present across the full latitudinal gradient.

The vegetation of three studied types of bogs (polygonal, flat-mound and ridge-hollow) is essentially oligotrophic (poor in nutrients) which indicates the ombrotrophic (rain and snow water fed) conditions, i.e., the lack of groundwater input and lateral surface influx of nutrients. The flat-mound palsa is covered by dwarf shrubs (*Ledum decumbens, Betula nana, Andromeda polifolia, Vaccinium ssp., Empetrum nigrum)*, lichens (*Cladonia ssp., Cetraria, Ochrolechia)* and mosses (*Dicranum ssp., Polytrichum ssp., Sphagnum angustifolium, S. lenense*). At southern sites, the pine *Pinus sylvestris* is abundant on ridges (Peregon et al., 2008, 2009) whereas the two taiga sites are dominated by *Pinus sylvestris f. uliginosa* with minor but permanently present *Betula pubescens* and *Pinus sibirica*. Dwarf shrubs are dominated by *Ledum palustre, Chamaedaphne calyculata, Vaccinium vitis-idaea.* The moss layer is dominated by *Sphagnum fuscum*, *S. angustifolium* with the presence of *Sphagnum magellanicum, S. capillifolium* and boreal forest moss species like *Pleurozium schreberi*.

2.2. Sampling procedure, analyses and data treatment

Peat core samples were collected in August, when the depth of unfrozen layer was at its maximum (i.e., see Raudina et al., 2017). Based on measurements by temperature loggers over the summer period, the in-situ temperature of studied soil profile ranged from 15±5°C in the top soil (0-20 cm) to 4±2°C at the permafrost boundary (40-80 cm). The physical, chemical and

https://doi.org/10.5194/bg-2019-483
Preprint. Discussion started: 28 January 2020

botanical properties of several peat cores collected in the homogeneous palsa region in the north and ridgre-ryam complex in the south are highly similar among different peat mounds (Velichko et al., 2011; Stepanova et al., 2015).

Peat cores were extracted using a Russian sediment/peat corer and the frozen part was sampled using a motorized Russian peat corer (UKB-12/25 I, Russia) with a 4-cm diameter corer sterilized with 40% ethanol prior to each extraction. We collected the full active (unfrozen) layer peat column, the frozen peat column and some 10 to 30 cm of frozen mineral horizons using clean powder-free vinyl gloves. Peat or mineral soil samples were divided in 5-10 cm segments using a sharp sterile single-use plastic knife. Soil samples were placed in sterile PVC doubled-zipped bags and kept at -20°C during transport and storage. To avoid contamination of peat from external surroundings, we separated the part of the core for geochemical analysis exclusively from the interior of the core (> 1 cm from the core liner) following conventional procedures (Wilhelm et al., 2011).

Total Hg concentration, THg, in freeze-dried and ground slices of peat cores was determined using a direct mercury analyzer (DMA-80 - Milestone, Italy). Analysis of reference material BCR-482 (lichen, 480±28 ng g^{-1}), MESS3 (sediment, 91±9 ng g^{-1}) and NIST 1632d (coal, 93±3 ng g^{-1}) showed good reproducibility (mean±1σ) of 467±28 ng g^{-1}, 80±6 ng g^{-1} and 98±8 ng g^{-1}, respectively. The average uncertainty on duplicate sample analysis did not exceed 5% (1σ). The carbon (C) and nitrogen (N) concentration were measured using catalytic combustion with Cu-O at 900°C with an uncertainty of ≤ 0.5% using Thermo Flash 2000 CN Analyzer, and aspartic acid (C 36.09%±1.5%; N 10.52%±0.5%) and soil SRM (C 2.29%±0.07%; N 0.21%±0.01%) as standards. Analyses of total C before and after sample treatment with HCl did not yield more than 1 % of inorganic C; therefore our total C-determination represents organic carbon. For trace and major element analysis, soil samples were subjected to full acid digestion in the clean room following ICP-MS (Agilent 7500 ce) analyses as described previously (Morgalev et al., 2017).

https://doi.org/10.5194/bg-2019-483
Preprint. Discussion started: 28 January 2020

The Shapiro Wilk normality test was used to asses THg, elemental and R_{HgC} distributions, and statistical data descriptors adjusted accordingly. All statistical tests used a significance level of 95% ($\alpha = 0.05$). Spearman rank order correlations (significant at $p < 0.05$) were performed to characterize the link of Hg with C, N and other major and trace elements. The differences in Hg concentration between the active- and frozen peat layer were tested using the Mann-Whitney U test for paired data at a significance level of 0.05.

C pools of different soil classes reported by Hugelius et al. (2014) were divided into two categories, organic and mineral soils. Histosols and Histels were defined as organic soils. Turbels and Orthels were considered as organic soils for the 0 – 0.3 m interval and as mineral soils for the 0.3 – 3m interval. All other soils were considered as mineral soils. To estimate the northern soil Hg pool, C pools were multiplied with the respective R_{HgC} derived for organic (>20% C) and mineral (<20% C) soil data from north America (excluding Alaska) and Eurasia. To calculate the global Hg pool, a simpler approach was used and one singe R_{HgC} was considered for 5 climate zones which were defined by latitude (arctic: > 67°, boreal: 50° - 67°, temperate: 35° - 50°, subtropical: 23.45° - 35°, tropical: <23.45°) according to FAO and ITPS (2018). The uncertainty was assessed with a Monte carlo approach using the *rnorm* and *rlnorm* function of R (version 3.6.1.) and is reported as the interquartile range (25th and 75th percentile) of 100,000 simulations. For the northern soil Hg pool, final uncertainties incorporate the uncertainties on the C stock from Hugelius et al. (2014) assuming normal distribution and uncertainties of R_{HgC} assuming log-normal distribution.

https://doi.org/10.5194/bg-2019-483
Preprint. Discussion started: 28 January 2020

Biogeosciences Discussions

3. Results

3.1. Depth (vertical) distribution of Hg in peat profiles

Hg concentration in peat cores of the WSL are illustrated in **Fig. 2** and primary data on soil chemical composition and Hg concentration are listed in **Table S2** of the Supplement. The upper 0-20 cm layer is 2 to 3 times enriched in Hg compared to the rest of the peat core in permafrost-affected sites (Khanymey, Pangody and Tazovsky). This is not the case, however, for the sporadic permafrost zone (Kogalym) and isolated permafrost zone (Mukhrino), where a local maximum at ca. 35 cm depth was detected but no enrichment of upper 10-20 cm horizons occurred. In the most southern, permafrost-free site of the WSL (Plotnikovo, southern taiga), the Hg concentration profile in the peat was fairly constant with a local minimum at 100 cm depth. The mean, depth-integrated Hg concentrations in active layer, permafrost and mineral horizons are illustrated in **Fig. 3** and summarized in **Table 1**. The latitudinal trend of Hg concentration in peat consists of a systematic increase northward, both in permafrost and active peat layers. The dominant ground vegetation (lichens) analyzed at 5 sites out of 6 (Plotnikovo, Kogalym, Khanymey, Pangody and Tazovsky) did not show significantly different (U test Mann-Whitney) Hg concentrations relative to the peat cores (**Fig. 3**). The typical concentrations of Hg in studied peat cores ranged from 7 to 284 ng g^{-1} with a median (± IQR) of 67±57 ng g^{-1}. The Hg concentration in the thawed, active layer was generally comparable to that in the frozen layer, supported by a Mann-Whitney test, which did not show significant difference in Hg concentration between frozen and thawed peat in all permafrost-affected sites. Within the latitudinal transect from south to north, the Hg concentrations in peat are higher (Plotnikovo, Kogalym, Khanymey, Pangody) or comparable (Tazovsky) to those in the mineral horizons.

The ratio of Hg:C (R_{HgC}, µg g^{-1}, corresponding to Gg Pg^{-1}) ranged between 0.05 and 2.0 over the peat columns, and was 5 to 10 times higher in mineral horizons compared to frozen peat and active layers (**Fig. 4**). The R_{HgC} in the active layer and in the mineral horizons increased 3-

fold from the south (56°N) to the north (67°N). In the frozen peat horizon, the R_{HgC} ratio increased two-fold from sporadic and isolated to continuous permafrost zone.

3.2. Regional and total pools of Hg in the WSL peat and mineral layers

The mass of Hg per area of soil in the active- and frozen peat layer as well as in the top 30 cm of frozen mineral horizons of the six studied WSL peat profiles was calculated by multiplying bulk soil peat and mineral layer densities (range from 0.01 to 0.38 g/cm^3, **Table S2**) by Hg concentration and integrating over the corresponding depths. The surface area - normalized Hg stock systematically increased from south to north (ca. 0.3 to 6.0 mg Hg m^{-2} and ca. 0.8 to 13.7 mg Hg m^{-2}, in the 0-30 and the 0-100 cm peat layer, respectively (**Fig. 5 A**). This northward increase was most pronounced for the active layer, was less evident for frozen peat, and insignificant for the upper 30 cm of mineral horizon located under the peat (**Fig. 5 B**). Taking into account the proportion of bogs (peatlands) in each zone (1° latitudinal grid) from Sheng et al. (2004), we calculated the pool of Hg in permafrost-free and permafrost-affected WSL peatlands (**Fig. 6**). The total pool of Hg in the 0-100 cm layer of peat bogs exhibits a maximum (356-580 Mg) in the discontinuous permafrost zone.

We estimate the total organic soil Hg pool in the WSL from the Hg stock (mg Hg m^{-2} over 0-100 cm depth) for permafrost and permafrost-free zones (**Fig. 7 A**), extrapolated to the full average thickness of peat in the WSL (280 cm, Sheng et al., 2004), assuming that Hg concentration in the upper 0-100 cm peat layer is the same as in 100-280 cm of peat and multiplied by the area of bogs in each latitudinal grid (S, m^2) as shown in **Fig 7 B**. This yields 1.7 Gg Hg in the permafrost-free zone and 7.6 Gg Hg in the permafrost-bearing zone with a total Hg pool of 9.3 Gg in the WSL. For this calculation we did not take into account the mineral horizons and we used variable active layer thickness across the latitudinal gradient of WSL, as estimated at our sampling sites (**Table S1**). The amount of Hg in permafrost-bearing zone within the active (unfrozen) peat

https://doi.org/10.5194/bg-2019-483
Preprint. Discussion started: 28 January 2020

layer (0-160 cm in the south and 0-20 cm in the north) of the WSL is 2.0 Gg, and that in the frozen (160-280 cm in the south and 20-280 cm in the north) layer) is 5.6 Gg.

Alternatively, to calculate the total pool of Hg in WSL bogs, we used the R_{HgC} inferred from our data across the gradient of permafrost and biomes (Table 1). Taking into account the C pool in the WSL (70.2 Pg C of 0-280 cm depth layer, Sheng et al., 2004) and the median R_{HgC} of 0.133 µg/g in the WSL, we calculated Hg for the full depth of the peat layer in each zone. This also gives 9.3 Gg Hg for a total area of 592,440 km².

3.3. Correlation of Hg with other elements in the peat cores

Spearman rank order correlations of Hg with other elements demonstrated significant positive relationships ($R > 0.60$; $p < 0.05$) with K, Rb, Cs, P, As, W, V, Cr, Cu in the active (unfrozen) layer (**Table S3** of Supplment). However, these relationships were less pronounced in the frozen peat, where only Mg, Ca, Sr, Mn, N, P, As, Cu, Ni, Sb and some REE demonstrated minor ($0.40 < R < 0.55$) positive correlations with Hg. Finally, in the mineral layer, significant ($R > 0.70$) positive correlations of Hg were observed with Li, Ca, Sr, P, N, Mn, Ni, Co, Cr, Cd. A positive ($R = 0.60$) relationship between Hg and C was observed in mineral horizons, whereas no correlation was detected in both frozen and thawed peat. This is consistent with some studies of peat soil in Brazil (Roulet et al., 1998) and Arctic tundra soils (Olson et al., 2018). At the same time, there was a positive correlation of Hg with N in the active layer, frozen peat and mineral horizons (R = 0.50, 0.47 and 0.75, respectively). Stronger and more stable correlation of Hg with N compared to C was also noted by Roulet (2000).

https://doi.org/10.5194/bg-2019-483
Preprint. Discussion started: 28 January 2020

4. Discussion

4.1. Hg association with other elements in peat

Stronger accumulation of Hg relative to C in mineral horizons in the north (Tazovsky**, Fig. 4**) may be linked to the clay nature of mineral layers (Roulet et al., 1998; Baptista-Salazar et al., 2017) in these regions (**Table S1**) but also to the presence of specific host phases of Hg (see examples of peat minerals in Rudmin et al., 2018). Dissolved oxygen measurements in soil porewaters at the Tazovsky site indicate that mineral gleysoils and peat histosols, which often overlay former lake sediments, are anoxic (Raudina et al., 2017; Loiko et al., 2019). The Hg host phases in these soils are therefore likely sulfide minerals. Indeed, known Hg carriers in peat deposits are Fe and Zn sulfide minerals or organic-bound sulfide functional groups (Smieja-Król et al., 2010; 2014; Prietzel et al., 2009; Skyllberg et al., 2003, Bates et al., 1998; Steinmann and Shotyk, 1997).

In the peat active layer, Hg was positively correlated with K, Rb, Cs, P, As, V, Cr, Cu (**Table S3**). In the frozen part of the peat core, Hg was positively correlated with Ca, N, Mn, Sr, Mg, P (**Table S3**). Indeed, atmospheric particles in snow across the WSL exhibit strong enrichment in Mo, W, As, Sb, Ni, Cu, Zn, Cd, Pb, Mg, Ca, and Na (Shevchenko et al., 2017). The strong positive correlation of Hg with these elements in peat soils of WSL suggests a common atmospheric origin. Note however, that the cited elements deposit with particles, rainfall and snowfall, whereas atmospheric Hg transfer to peat occurs mainly via the vegetation pump, with tundra and taiga vegetation actively taking up atmospheric gaseous Hg^0 through foliage (Obrist et al., 2017; Jiskra et al., 2018).

4.2. Estimating the northern soil Hg pool

A recent study used a median R_{HgC} value of 1.6 µg g^{-1}, observed mainly in mineral soil samples (median SOC of 3%, IQR=1.7 to 8.7 %) along a transect in Alaska, to estimate a northern permafrost soil Hg pool of 755±427 Gg in the upper 0-100 cm, and 1656±962 Gg in the upper 0-300 cm (Schuster et al. 2018). In the case of western Siberia, this high R_{HgC} value overestimates the Hg pool 12-fold, given that the median R_{HgC} in WSL peat is only 0.13±0.12 (median±IQR) (**Table 1, Fig. 4**). The extrapolation based on Alaskan R_{HgC} for the whole Northern Hemisphere permafrost region also suggests that the WSL contains large amounts of Hg in the upper 0-30 cm (20-40 mg Hg m^{-2}) and in the upper 0-100 cm (40-80 mg Hg m^{-2}). These numbers are much higher than the direct measurements in this study: 0.3 mg Hg m^{-2} in 0-30 cm and 0.8-1.3 mg Hg m^{-2} in 0-100 cm layer in the permafrost-free zone (Plotnikovo and Mukhrino sites); 0.5 mg Hg m^{-2} in 0-30 cm and 3.0 mg Hg m^{-2} in 0-100 cm layer in the sporadic zone (Kogalym site); 1.8-4.0 mg Hg m^{-2} in 0-30 cm and 9.6-11.9 mg Hg m^{-2} in 0-100 cm layer in the continuous to discontinuous permafrost zone (Khanymey and Pangody sites), and 6.0 mg Hg m^{-2} in 0-30 cm and 13.7 mg Hg m^{-2} in 0-100 cm layer in continuous permafrost zone (Tazovsky). It is worth noting that the recent data of Talbot et al. (2017) for Ontario (Canada) bogs (S_{area} = 1,133,990 km²; 18.8 Gg Hg for the 277 ± 123 cm depth) are consistent with the results of the present study in the WSL (9.3 Gg Hg for 592,440 km² for the 280 ± 100 cm depth).

A revised value of the Hg pool in the northern soils was recently provided by Olson et al. (2018) who combined measured R_{HgC} values for Alaskan tundra soils with literature data, and derived R_{HgC} of 0.12 µg g^{-1} for 0-30 cm (organic) and 0.62 µg g^{-1} for 30-100 cm (mineral) layers. Olson et al. (2018) estimate northern permafrost soil Hg pools of 26 Gg (0-30 cm) and 158 Gg (30-100 cm), which combined (184 Gg) is 4 times lower than the number of 755 Gg (0-100 cm) by Schuster et al. (2014). Both studies rely on R_{HgC} measurements from Alaskan soils, due to relatively easy road access to the sampling sites along the Dalton Highway. Bedrock along the Dalton Highway contains relatively high geogenic Hg levels (mean concentration: 32 ng/g), resulting in a high geogenic contribution in mineral soils (39% for B horizons and 20% for A horizons, Obrist et al., 2017). As a result, R_{HgC} in mineral soils along the Dalton highway are

https://doi.org/10.5194/bg-2019-483
Preprint. Discussion started: 28 January 2020

Biogeosciences Discussions
Open Access

higher (median = 1.6, Schuster et al. 2018) than for other mineral soils in North Amercia and Eurasia (median = 0.64, **Figure 8**). It is clear that any upscaling calculation of pan-Arctic permafrost Hg depends critically on the R_{HgC} of the 0-30 and 30-100 cm peat layers, as Eurasian sporadic to continuous permafrost represents 54% of the northern soil C inventory (**Table 2**). Compared to the previously assumed R_{HgC} of 1.6 (Schuster et al. 2018), and 0.12 - 0.62 µg g^{-1} (Olson et al.., 2018), we observe lower R_{HgC} ranging from 0.065 to 0.38 µg g^{-1} at 0-100 cm depth. Setting Alaska aside as a geographic region, we find that North American and Eurasian mineral (<20% SOC) soil R_{HgC} was lower (μ = 0.77 µg g^{-1}, median= 0.63 µg g^{-1} (IQR = 0.32 to 0.80 µg g^{-1}), n=131) than R_{HgC} reported for Alaska (median= 1.64 µg g^{-1} (IQR = 0.91 to 2.93 µg g^{-1}), n=589) (**Figure 8**). The R_{HgC} in organic soils (>20% SOC, including data from Alaska) was approximately 4 times lower (μ= 0.19 µg g^{-1}, median= 0.15 µg g^{-1} (IQR = 0.09 to 0.24 µg g^{-1}), n=449) than that in mineral soils of North America and Eurasia (**Figure 8**), consistent with the observed difference in WSL mineral and organic soils. Higher R_{HgC} observed in mineral soils may originate from a contribution of geogenic Hg from the weathered bedrock (independent of C stock) and/or a higher mineralization rate of C (preferential C over Hg loss) in predominantly oxic mineral soils compared to anoxic peat soils.

In **Table 2** we revisit the full 0-300 cm northern permafrost soil Hg inventory, based on N-American (excluding Alaska) and Eurasian R_{HgC} based on the literature data compilations of Olson et al. (2018) and Schuster et al. (2018), and our observed WSL R_{HgC} for Eurasia, multiplied by estimated northern tundra soil organic C pools for 0-300 cm from and Hugelius et al. (2014). The error made by neglecting high R_{HgC} in Alaskan mineral soils is small, on the order of 2.5 Gg Hg, as estimated from the relatively small Alaskan C pool of 2.6 Pg C (Tarnocai et al., 2009). We estimate the northern soil Hg pool to be 67 Gg (37-88 Gg, IQR) in the upper 30 cm, 225 Gg (102-320 Gg) in the upper 1 m, and 557 Gg (371-699 Gg) in the upper 3 m (**Table 3**). Note that our revised values in the 0 - 1m range (225 Gg) is similar to that of Olson et al. (184 Gg), but lower

https://doi.org/10.5194/bg-2019-483
Preprint. Discussion started: 28 January 2020

than that of Schuster et al. (755 Gg). We find that Hg stocks in organic soils (>20% SOC) represent 56% and 21% of the total Hg stock in the 0-30 cm and 0-100 cm depth range, respectively (**Table 2**). The rest of the pan-arctic Hg is associated with C in mineral soils (<20% SOC) for which relatively sparse data exists (n=131). In particular, turbel and orthel mineral soils, which are estimated to contain 49 to 62% of total arctic C (Hugelius et al., 2014) and 36 to 85% of Hg at the various depth intervals need to be further investigated.

4.3. Estimating the global soil (0-30 cm) Hg pool

To estimate the global soil Hg pool, we combined the more detailed Arctic pool estimate (separating organic and mineral soils) with a more basic approach for the other climate zones, where we derived bulk R_{HgC} for the 0-30 cm surface soils based on published literature data and multiplied it with global C stock estimates for each climate zone (arctic, boreal, temperate, subtropical and tropical) from the global soil organic carbon map (FAO and ITPS, 2018). The R_{HgC} increases from cold climate zones to warmer climate, from 0.15 µg g^{-1} for Arctic organic soils, to 1.8 µg g^{-1} in subtropical and tropical soils (**Figure 9, Table 4**). This latitudinal trend in R_{HgC} likely reflects a combination of low C mineralization rates in colder north and additional Hg sorption to Fe(oxy)hidroxides in old tropical soils. Taking into account the variation in R_{HgC} and C stocks across the climate zones, we estimate a global Hg stock of 1084 Gg (848 – 1258 Gg, IQR) for the top 0 - 30 cm (**Table 4**). Previous global Hg soil pool estimates vary between 232 and 1150 Gg (Selin et al., 2008; Smith-Downey et al., 2010; Amos et al., 2013, 2015; Hararuk et al., 2013; Wang et al., 2019). Schuster et al. (2018) concluded that Arctic permafrost soils store nearly twice the amount of Hg as all other soils, the Ocean and atmosphere combined, but in doing so they compared different global (0 - 30cm) and Arctic soil depth ranges (0 - 300cm). Our revised estimate of the pan-Arctic permafrost and global soil pool suggests that, for a similar depth range of 0-30 cm, permafrost soils contain 6% (67 Gg) of the global soil Hg pool (1084 Gg).

https://doi.org/10.5194/bg-2019-483
Preprint. Discussion started: 28 January 2020

4.4. Northern soil Hg sequestration and Hg loss

Olson et al. (2018) recognized that the large 0-100 cm northern soil Hg pool is the result of thousands of years of net atmospheric Hg deposition. The latitudinal trend of northward increasing peat Hg concentration in the WSL (**Fig. 4, 5**) illustrates that this net Hg deposition is a fine balance between the vegetation Hg pump, which sequesters Hg^0 in soils via foliar uptake and litterfall, and Hg^0 emission during biomass decay of vegetation debris. Annual gross Hg sequestration by vegetation, via the vegetation pump, likely scales with primary productivity and therefore decreases northward as insolation and growing season decrease. However, in the north, degradation rates of vegetation biomass are lower than in the south: the moss biomass losses during decomposition in the forest tundra zone (5-6% over 1st year and 10-12% over 2 years) is lower than that in the southern taiga (10-20% over 1st year and 20-40% over 2 years), based on in-situ biomass degradation experiments across the WSL gradient of biomes (Vishnyakova and Mironycheva-Tokareva, 2018). The net result is a higher preservation of soil Hg in the north, where less emission of Hg^0 during plant decay occurs. The dependence of this balance, between Hg^0 sequestration and Hg^0 re-emission, on climate explains qualitatively the contrasting observations made in Toolik (AK, USA, 68°N, MAAT = -7°C, Obrist et al., 2017) and Degerö Stormyr (Sweden, 64°N, MAAT = 2°C, Osterwalder et al., 2018). At Toolik, net Hg^0 deposition by vegetation and soil uptake occurs on an annual basis, whereas at Degerö Stormyr higher temperatures result in net annual Hg^0 emission. More research is needed to quantify the climate dependence of Hg^0 sequestration (as soil Hg^{II}) and Hg^0 re-emission before we can predict and model northern soil Hg loss to the atmosphere due to global warming trajectories.

https://doi.org/10.5194/bg-2019-483
Preprint. Discussion started: 28 January 2020

5. Conclusions

Western Siberian peatlands contain a large amount of Hg in frozen and thawed peat; the lateral pools of peat palsa bogs range from 1-2 mg Hg m^{-2} in the south to 10-15 mg Hg m^{-2} in the north. This northward increase of Hg concentration and pools can be explained by better preservation of organic-bound Hg due to colder temperatures and shorter active period in the continuous permafrost zone compared to the discontinuous and sporadic zones. We revisited the full 0-300 cm northern permafrost soil Hg inventory, based on published R_{HgC} and our observed WSL R_{HgC} for Eurasia, together with estimated northern tundra soil organic C pools for 0-300 cm from Hugelius et al. (2014). We estimate the 0-300 cm northern permafrost soil Hg inventory to be 557 Gg (371-699 Gg, IQR), which is three times lower than a previous estimate of 1656 ± 962 Gg Hg for the same depth range (Schuster et al., 2018). We estimate the global soil Hg pool to be 1084 Gg for the 0-30cm depth range. The permafrost Hg pool for the same 0 - 30cm depth range is 67 Gg, and while large compared to the 3 Gg of Hg residing in the Arctic Ocean (Soerensen et al., 2016), it represents only 6% of the global soil Hg pool.

Data availability. Hg and C concentration data of the WSL soil samples are available in the supplement. The permafrost data from Schuster et al. 2018 and a global compilation of R_{HgC} data is available as supplementary information (https://agupubs.onlinelibrary.wiley.com/doi/full/10.1002/2017GL075571, last access: 6 December 2019). The data from the Olson et al. 2018 study is available from the corresponding author upon request. The data from the tropical climate zone was compiled from original publications of Almeida (2005); Almeida et al. (2005); Campbell et al. (2003); Melendez-Perez et al. (2014).

Author contributions. OSP and SVL designed the study. SVL, AGL, and NK performed field sampling. AGL and OSP did all laboratory analysis. MJ and JES did the northern soil and global soil Hg pool calculations. All authors contributed to writing of the manuscript.

We declare no competing interests

Acknowledgements:

This work was mainly supported by the state task of the Ministry of Science and Higher Education of the Russian Federation, grant no. 1.8195.2017/P220. Partial support from the Russian Fund for Basic Research, via grant no. 19-29-05209-mk and 19-55-15002-NCNI_a, and from the CNRS Chantier Arctique Français, via the PARCS project, and the H2020 ERA-PLANET (689443) iGOSP and iCUPE programmes are acknowledged. M.J. acknowledges funding by the Swiss National Science Foundation (grant no. PZ00P2_174101). We are thankful to Luiz D. Lacerda for sharing Hg and C data from Brazil.

References

Almeida, M. D., Lacerda, L. D., Bastos, W. R., and Herrmann, J. C.: Mercury loss from soils following conversion from forest to pasture in Rondônia, Western Amazon, Brazil, Environ. Pollut., 137(2), 179–186, doi:10.1016/j.envpol.2005.02.026, 2005.

Almeida, M.D.: Biogeoquímica de mercúrio na interface solo-atmosfera na Amazônia, Ph.D. thesis, Univsidade Federal Fluminense, Niterói, Brazil, 221 pp., 2005.

Amos, H. M., Jacob, D. J., Kocman, D., Horowitz, H. M., Zhang, Y., Dutkiewicz, S., Horvat, M., Corbitt, E. S., Krabbenhoft, D. P., and Sunderland, E. M.: Global biogeochemical implications of mercury discharges from rivers and sediment burial, Environ. Sci. Technol., 48(16), 9514–9522, doi:10.1021/es502134t, 2014.

Amos, H. M., Sonke, J. E., Obrist, D., Robins, N., Hagan, N., Horowitz, H. M., Mason, R. P., Witt, M., Hedgecock, I. M., Corbitt, E. S., and Sunderland, E. M.: Observational and Modeling Constraints on Global Anthropogenic Enrichment of Mercury, Environ. Sci. Technol., 49(7), 4036–4047, doi:10.1021/es5058665, 2015.

Anisimov, O. A., and Sherstiukov, A. B.: Evaluating the effect of climatic and environmental factors on permafrost in Russia, Earth's Cryosphere, XX (2), 78-86, 2016.

Anisimov, O., and Reneva, S.: Permafrost and changing climate: the Russian perspective, AMBIO: A Journal of the Human Environment. 35(4), 169-176, https://doi.org/10.1579/0044-7447(2006)35[169:PACCTR]2.0.CO;2, 2006.

Bailey, E. A., Gray, J. E., and Theodorakos, P. M.: Mercury in vegetation and soils at abandoned mercury mines in southwestern Alaska, USA, Geochemistry Explor. Environ. Anal., 2(3), 275–285, doi:10.1144/1467-787302-032, 2002.

Baptista-Salazar, C., Richard, J. H., Horf, M., Rejc, M., Gosar, M., and Biester, H.: Grain-size dependence of mercury speciation in river suspended matter, sediments and soils in a mercury mining area at varying hydrological conditions, Appl. Geochemistry, 81, 132–142, doi:10.1016/j.apgeochem.2017.04.006, 2017.

Bates, A. L., Spiker, E. C., and Holmes, C. W.: Speciation and isotopic composition of sedimentary sulfur in the Everglades, Florida, USA, Chem. Geol., 146(3–4), 155–170, doi:10.1016/S0009-2541(98)00008-4, 1998.

Bedritsky, A.I.: Global climate and soil cover Russia: estimation of risks and environmental and econoical consequences of land degradation. Adaptive systems and technologies of agriculture and forestry, Moscow, National report, 2018. (In Russian).

Brown, J., Ferrians Jr, O. J., Heginbottom, J. A., and Melnikov, E. S.: Circum-arctic map of permafrost and ground ice conditions, National Snow and Ice Data Center, Digital media, Boulder, CO 80309-0449 USA, 1998, revised February 2001.

Campbell, L. M., Hecky, R. E., Muggide, R., Dixon, D. G., and Ramlal, P. S.: Variation and distribution of total mercury in water, sediment and soil from northern Lake Victoria, East Africa, Biogeochemistry, 65(2), 195–211, doi:10.1023/A:1026058417584, 2003.

Dastoor, A. P., and Durnford, D. A.: Arctic Ocean: Is It a Sink or a Source of Atmospheric Mercury?, Environ. Sci. Technol., 48(3), 1707–1717, doi:10.1021/es404473e, 2014.

Fahnestock, M. F., Bryce, J. G., McCalley, C. K., Montesdeoca, M., Bai, S., Li, Y., Driscoll, C. T., Crill, P. M., Rich, V. I., and Varner, R. K.: Mercury reallocation in thawing subarctic peatlands, Geochemical Perspect. Lett., 6, doi:10.7185/geochemlet.1922, 2019.

FAO and ITPS: Global Soil Organic Carbon Map (GSOCmap), Technical Report, Rome, 162 pp. 2018.

Fisher, J. A., Jacob, D. J., Soerensen, A. L., Amos, H. M., Steffen, A., and Sunderland, E. M.: Riverine source of Arctic Ocean mercury inferred from atmospheric observations, Nat. Geosci., 5(7), 499–504, doi:10.1038/ngeo1478, 2012.

Frey, K. E., McClelland, J. W., Holmes, R. M., and Smith, L. G.: Impacts of climate warming and permafrost thaw on the riverine transport of nitrogen and phosphorus to the Kara Sea, J. Geophys. Res. Biogeosciences, 112(4), doi:10.1029/2006JG000369, 2007.a

Frey, K. E., Siegel, D. I., and Smith, L. C.: Geochemistry of west Siberian streams and their potential response to permafrost degradation, Water Resour. Res., 43(3), doi:10.1029/2006WR004902, 2007.b

Golovatskaya, E. A., and Lyapina, E. E.: Distribution of total mercury in peat soil profiles in West Siberia, Contemp. Probl. Ecol., 2(2), 156–161, doi:10.1134/S199542550902012X, 2009.

Hararuk, O., Obrist, D., and Luo, Y.: Modelling the sensitivity of soil mercury storage to climate-induced changes in soil carbon pools, Biogeosciences, 10(4), 2393–2407, doi:10.5194/bg-10-2393-2013, 2013.

Hugelius, G., Strauss, J., Zubrzycki, S., Harden, J. W., Schuur, E. A. G., Ping, C. L., Schirrmeister, L., Grosse, G., Michaelson, G. J., Koven, C. D., O'Donnell, J. A., Elberling, B., Mishra, U., Camill, P., Yu, Z., Palmtag, J., and Kuhry, P.: Estimated stocks of circumpolar permafrost carbon with quantified uncertainty ranges and identified data gaps, Biogeosciences, 11(23), 6573–6593, doi:10.5194/bg-11-6573-2014, 2014.

Jensen, A., and Jensen, A.: Historical deposition rates of mercury in scandinavia estimated by dating and measurement of mercury in cores of peat bogs, Water, Air, Soil Pollut., 56(1), 769–777, doi:10.1007/BF00342315, 1991.

Jiskra, M., Sonke, J. E., Agnan, Y., Helmig, D., and Obrist, D.: Insights from mercury stable isotopes on terrestrial–atmosphere exchange of Hg(0) in the Arctic tundra, Biogeosciences, 16(20), 4051–4064, doi:10.5194/bg-16-4051-2019, 2019.

Jiskra, M., Sonke, J. E., Obrist, D., Bieser, J., Ebinghaus, R., Myhre, C. L., Pfaffhuber, K. A., Wängberg, I., Kyllönen, K., Worthy, D., Martin, L. G., Labuschagne, C., Mkololo, T.,

https://doi.org/10.5194/bg-2019-483
Preprint. Discussion started: 28 January 2020

Ramonet, M., Magand, O., and Dommergue, A.: A vegetation control on seasonal variations in global atmospheric mercury concentrations, Nat. Geosci., 11(4), 244–250, doi:10.1038/s41561-018-0078-8, 2018.

Kremenetski, K. V., Velichko, A. A., Borisova, O. K., MacDonald, G. M., Smith, L. C., Frey, K. E., and Orlova, L. A.: Peatlands of the Western Siberian lowlands: Current knowledge on zonation, carbon content and Late Quaternary history, Quat. Sci. Rev., 22(5–7), 703–723, doi:10.1016/S0277-3791(02)00196-8, 2003.

Kurina, I.V., and Veretennikova, E.E.: Impact of climate change of the Holocene on the development of the ridge-hollow swamp complex of Western Siberia, Izvestiya Rossiiskoi Akademii Nauk, Seriya Geograficheskaya, 2, 74-87, https://doi.org/10.15356/0373-2444-2015-2-74-87, 2015. (In Russian).

Kurina, I.V., Veretennikova, E.E., Il'ina, A.A., Dyukarev, E.A., Golovatskaya, E.A., and Smirnov, S.V.: Reconstruction of conditions of formation of the eutrophic peatland deposits in south of the taiga zone of Western Siberia, Izvestiya Rossiiskoi Akademii Nauk, Seriya Geograficheskaya, 4, 66-76, https://doi.org/10.1134/S2587556618040106, 2018.

Lim, A. G., Sonke, J. E., Krickov, I. V., Manasypov, R. M., Loiko, S. V., and Pokrovsky, O. S.: Enhanced particulate Hg export at the permafrost boundary, western Siberia, Environ. Pollut., 254, doi:10.1016/j.envpol.2019.113083, 2019.

Loiko, S., Raudina, T., Lim, A., Kuzmina, D., Kulizhskiy, S., and Pokrovsky, O.: Microtopography Controls of Carbon and Related Elements Distribution in the West Siberian Frozen Bogs, Geosciences, 9(7), 291, doi:10.3390/geosciences9070291, 2019.

Lyapina, E. E., Golovatskaya, E. A., and Ippolitov, I. I.: Mercury concentration in natural objects of west Siberia, Contemp. Probl. Ecol., 2(1), 1–5, doi:10.1134/S1995425509010019, 2009.

Melendez-Perez, J. J., Fostier, A. H., Carvalho, J. A., Windmöller, C. C., Santos, J. C., and Carpi, A.: Soil and biomass mercury emissions during a prescribed fire in the Amazonian rain forest, Atmos. Environ., 96, 415–422, doi:10.1016/j.atmosenv.2014.06.032, 2014.

Morel, F. M. M., Kraepiel, A. M. L., and Amyot, M.: The chemical cycle and bioaccumulation of mercury, Annu. Rev. Ecol. Syst., 29, 543–566, doi:10.1146/annurev.ecolsys.29.1.543, 1998.

Morgalev, Y. N., Lushchaeva, I. V., Morgaleva, T. G., Kolesnichenko, L. G., Loiko, S. V., Krickov, I. V., Lim, A., Raudina, T. V., Volkova, I. I., Shirokova, L. S., Morgalev, S. Y., Vorobyev, S. N., Kirpotin, S. N., and Pokrovsky, O. S.: Bacteria primarily metabolize at the active layer/permafrost border in the peat core from a permafrost region in western Siberia, Polar Biol., 40(8), 1645–1659, doi:10.1007/s00300-017-2088-1, 2017.

Nadyozhina, E.D., Shkolnik, I.M., Pavlova, T.V., Molkentin, E.K., and Semioshina, A.A.: Permafrost response to the climate warming as simulated by the regional climate model of the main geophysical observatory, Earth's Cryosphere, XII 3, 3–11, 2008. (In Russian).

Obrist, D., Agnan, Y., Jiskra, M., Olson, C. L., Colegrove, D. P., Hueber, J., Moore, C. W., Sonke, J. E., and Helmig, D.: Tundra uptake of atmospheric elemental mercury drives Arctic mercury pollution, Nature, 547(7662), 201–204, doi:10.1038/nature22997, 2017.

Olson, C., Jiskra, M., Biester, H., Chow, J., and Obrist, D.: Mercury in Active-Layer Tundra Soils of Alaska: Concentrations, Pools, Origins, and Spatial Distribution, Global Biogeochem. Cycles, 32(7), 1058–1073, doi:10.1029/2017GB005840, 2018.

Osterwalder, S., Sommar, J., Åkerblom, S., Jocher, G., Fritsche, J., Nilsson, M. B., Bishop, K., and Alewell, C.: Comparative study of elemental mercury flux measurement techniques over a Fennoscandian boreal peatland, Atmos. Environ., 172, 16–25, doi:10.1016/j.atmosenv.2017.10.025, 2018.

Outridge, P. M., Macdonald, E. R. W., Wang, G. F., Stern, G. A., and Dastoor, A. P.: A mass balance inventory of mercury in the Arctic Ocean, Environ. Chem, 5, 89–111, doi:10.1071/EN08002, 2008.

Panova, N. K., Trofimova, S. S., Antipina, T. G., Zinoviev, E. V., Gilev, A. V., and Erokhin, N. G.: Holocene dynamics of vegetation and ecological conditions in the southern Yamal Peninsula according to the results of comprehensive analysis of a relict peat bog deposit, Russ. J. Ecol., 41(1), 20–27, doi:10.1134/S1067413610010042, 2010.

Pavlov, A.V., and Malkova, G.V.: Mapping of trends of the contemporary ground temperature changes in the Russian north, Earth's Cryosphere, XIII 4, 32–39, 2009. (In Russian).

Pearson, C., Howard, D., Moore, C., and Obrist, D.: Mercury and trace metal wet deposition across five stations in Alaska: controlling factors, spatial patterns, and source regions, Atmos. Chem. Phys., 19(10), 6913–6929, doi:10.5194/acp-19-6913-2019, 2019.

Peregon, A., Maksyutov, S., and Yamagata, Y.: An image-based inventory of the spatial structure of West Siberian wetlands, Environ. Res. Lett., 4(4), doi:10.1088/1748-9326/4/4/045014, 2009.

Peregon, A., Maksyutov, S., Kosykh, N. P., and Mironycheva-Tokareva, N. P.: Map-based inventory of wetland biomass and net primary production in western Siberia, J. Geophys. Res. Biogeosciences, 113(1), doi:10.1029/2007JG000441, 2008.

Pokrovsky, O. S., Manasypov, R. M., Loiko, S. V., Krickov, I. A., Kopysov, S. G., Kolesnichenko, L. G., Vorobyev, S. N., and Kirpotin, S. N.: Trace element transport in western Siberian rivers across a permafrost gradient, Biogeosciences, 13(6), 1877–1900, doi:10.5194/bg-13-1877-2016, 2016.

Pokrovsky, O. S., Manasypov, R. M., Loiko, S., Shirokova, L. S., Krickov, I. A., Pokrovsky, B. G., Kolesnichenko, L. G., Kopysov, S. G., Zemtzov, V. A., Kulizhsky, S. P., Vorobyev, S. N., and Kirpotin, S. N.: Permafrost coverage, watershed area and season control of dissolved carbon and major elements in western Siberian rivers, Biogeosciences, 12(21), 6301–6320, doi:10.5194/bg-12-6301-2015, 2015.

Ponomareva, O.E., Gravis, A.G., and Berdnikov, N.M.: Contemporary dynamics of frost mounds and flat peatlands in north taiga of West Siberia (on the example of Nadym site), Earth's Cryosphere, 16, 21–30, 2012. (In Russian).

Preis, Y., and Karpenko, L.V.: Detailed reconstruction of bog functional state as a response to continental climate changes in Holocene (the middle taiga of Western Siberia), Bulletin of the Tomsk Polytechnic University, Geo Assets Engineering, 326 (2), 90-102, 2015. (In Russian).

Prietzel, J., Tyufekchieva, N., Eusterhues, K., Kögel-Knabner, I., Thieme, J., Paterson, D., McNulty, I., de Jonge, M., Eichert, D., and Salomé, M.: Anoxic versus oxic sample pretreatment: Effects on the speciation of sulfur and iron in well-aerated and wetland soils as assessed by X-ray absorption near-edge spectroscopy (XANES), Geoderma, 153(3–4), 318–330, doi:10.1016/j.geoderma.2009.08.015, 2009.

Raudina, T. V., Loiko, S. V., Lim, A. G., Krickov, I. V., Shirokova, L. S., Istigechev, G. I., Kuzmina, D. M., Kulizhsky, S. P., Vorobyev, S. N., and Pokrovsky, O. S.: Dissolved organic carbon and major and trace elements in peat porewater of sporadic, discontinuous, and continuous permafrost zones of western Siberia, Biogeosciences, 14(14), 3561–3584, doi:10.5194/bg-14-3561-2017, 2017.

Romanovsky, V. E., Smith, S. L., and Christiansen, H. H.: Permafrost thermal state in the polar Northern Hemisphere during the international polar year 2007–2009: a synthesis, Permafrost periglac, 21(2), 106-116, https://doi.org/10.1002/ppp.683, 2010.

Romanovsky, V.E., Kholodov, A.L., Marchenko, S.S., Oberman, N.G., Drozdov, D.S., Malkova, G.V., Moskalenko, N.G., Vasiliev, A. A., Sergeev, D. O., and Zheleznyak, M. N.: Thermal State and Fate of Permafrost in Russia: First Results of IPY, in: Proceedings of the 9th

https://doi.org/10.5194/bg-2019-483
Preprint. Discussion started: 28 January 2020

International Conference on Permafrost, edited by: Kane, D.L., and Hinkel, K.M., University of Alaska, Fairbanks, June 29 – July 3, 2008 , vol. 2, 1511–1518, 2008.

Roulet, M., Lucotte, M., Canuel, R., Farella, N., Courcelles, M., Guimarães, J. R. D., Mergler, D., and Amorim, M.: Increase in mercury contamination recorded in lacustrine sediments following deforestation in the central Amazon, Chem. Geol., 165(3–4), 243–266, doi:10.1016/S0009-2541(99)00172-2, 2000.

Roulet, M., Lucotte, M., Saint-Aubin, A., Tran, S., Rhéault, I., Farella, N., De Jesus Da Silva, E., Dezencourt, J., Sousa Passos, C. J., Santos Soares, G., Guimarães, J. R. D., Mergler, D., and Amorim, M.: The geochemistry of mercury in central Amazonian soils developed on the Alter-do-Chao formation of the lower Tapajos River Valley, Para state, Brazil, Sci. Total Environ., 223(1), 1–24, doi:10.1016/S0048-9697(98)00265-4, 1998.

Rudmin, M., Ruban, A., Savichev, O., Mazurov, A., Dauletova, A., and Savinova, O.: Authigenic and detrital minerals in peat environment of vasyugan swamp, western Siberia, Minerals, 8(11), doi:10.3390/min8110500, 2018.

Rydberg, J., Klaminder, J., Rosén, P., and Bindler, R.: Climate driven release of carbon and mercury from permafrost mires increases mercury loading to sub-arctic lakes, Sci. Total Environ., 408(20), 4778–4783, doi:10.1016/j.scitotenv.2010.06.056, 2010.

Schuster, P. F., Schaefer, K. M., Aiken, G. R., Antweiler, R. C., Dewild, J. F., Gryziec, J. D., Gusmeroli, A., Hugelius, G., Jafarov, E., Krabbenhoft, D. P., Liu, L., Herman-Mercer, N., Mu, C., Roth, D. A., Schaefer, T., Striegl, R. G., Wickland, K. P., and Zhang, T.: Permafrost Stores a Globally Significant Amount of Mercury, Geophys. Res. Lett., 45(3), 1463–1471, doi:10.1002/2017GL075571, 2018.

Selin, N. E., Jacob, D. J., Yantosca, R. M., Strode, S., Jaeglé, L., and Sunderland, E. M.: Global 3-D land-ocean-atmosphere model for mercury: Present-day versus preindustrial cycles and anthropogenic enrichment factors for deposition, Global Biogeochem. Cycles, 22(2), doi:10.1029/2007GB003040, 2008.

Sheng, Y., Smith, L. C., MacDonald, G. M., Kremenetski, K. V., Frey, K. E., Velichko, A. A., Lee, M., Beilman, D. W., and Dubinin, P.: A high-resolution GIS-based inventory of the west Siberian peat carbon pool, Global Biogeochem. Cycles, 18(3), doi:10.1029/2003GB002190, 2004.

Shevchenko, V. P., Pokrovsky, O. S., Vorobyev, S. N., Krickov, I. V., Manasypov, R. M., Politova, N. V., Kopysov, S. G., Dara, O. M., Auda, Y., Shirokova, L. S., Kolesnichenko, L. G., Zemtsov, V. A., and Kirpotin, S. N.: Impact of snow deposition on major and trace element concentrations and elementary fluxes in surface waters of the Western Siberian Lowland across a 1700'km latitudinal gradient, Hydrol. Earth Syst. Sci., 21(11), 5725–5746, doi:10.5194/hess-21-5725-2017, 2017.

Skyllberg, U., Qian, J., Frech, W., Xia, K., and Bleam, W. F.: Distribution of mercury, methyl mercury and organic sulphur species in soil, soil solution and stream of a boreal forest catchment, Biogeochemistry, 64(1), 53–76, doi:10.1023/A:1024904502633, 2003.

Smieja-Król, B., Fiałkiewicz-Kozieł, B., Sikorski, J., and Palowski, B.: Heavy metal behaviour in peat - A mineralogical perspective, Sci. Total Environ., 408(23), 5924–5931, doi:10.1016/j.scitotenv.2010.08.032, 2010.

Smith-Downey, N. V, Sunderland, E. M., and Jacob, D. J.: Anthropogenic impacts on global storage and emissions of mercury from terrestrial soils: Insights from a new global model, J. Geophys. Res., 115(G3), G03008, doi:10.1029/2009JG001124, 2010.

Soerensen, A. L., Jacob, D. J., Schartup, A. T., Fisher, J. A., Lehnherr, I., St Louis, V. L., Heimbürger, L. E., Sonke, J. E., Krabbenhoft, D. P., and Sunderland, E. M.: A mass budget for mercury and methylmercury in the Arctic Ocean, Global Biogeochem. Cycles, 30(4), 560–575, doi:10.1002/2015GB005280, 2016.

https://doi.org/10.5194/bg-2019-483
Preprint. Discussion started: 28 January 2020

Biogeosciences Discussions Open Access EGU

Sonke, J. E., Teisserenc, R., Heimbürger-Boavida, L. E., Petrova, M. V., Marusczak, N., Le Dantec, T., Chupakov, A. V., Li, C., Thackray, C. P., Sunderland, E. M., Tananaev, N., and Pokrovsky, O. S.: Eurasian river spring flood observations support net Arctic Ocean mercury export to the atmosphere and Atlantic Ocean, Proc. Natl. Acad. Sci. U. S. A., 115(50), E11586–E11594, doi:10.1073/pnas.1811957115, 2018.

St. Pierre, K. A., St. Louis, V. L., Lehnherr, I., Gardner, A. S., Serbu, J. A., Mortimer, C. A., Muir, D. C. G., Wiklund, J. A., Lemire, D., Szostek, L., and Talbot, C.: Drivers of Mercury Cycling in the Rapidly Changing Glacierized Watershed of the High Arctic's Largest Lake by Volume (Lake Hazen, Nunavut, Canada), Environ. Sci. Technol., 53(3), 1175–1185, doi:10.1021/acs.est.8b05926, 2019.

Steffen, A., Douglas, T., Amyot, M., Ariya, P., Aspmo, K., Berg, T., Bottenheim, J., Brooks, S., Cobbett, F., Dastoor, A., Dommergue, A., Ebinghaus, R., Ferrari, C., Gardfeldt, K., Goodsite, M. E., Lean, D., Poulain, A. J., Scherz, C., Skov, H., Sommar, J., and Temme, C.: A synthesis of atmospheric mercury depletion event chemistry in the atmosphere and snow, Atmos. Chem. Phys., 8(6), 1445–1482, doi:10.5194/acp-8-1445-2008, 2008.

Steinmann, P., and Shotyk, W.: Chemical composition, pH, and redox state of sulfur and iron in complete vertical porewater profiles from two Sphagnum peat bogs, Jura Mountains, Switzerland, Geochim. Cosmochim. Acta, 61(6), 1143–1163, doi:10.1016/S0016-7037(96)00401-2, 1997.

Stepanova, V. A., Pokrovsky, O. S., Viers, J., Mironycheva-Tokareva, N. P., Kosykh, N. P., and Vishnyakova, E. K.: Elemental composition of peat profiles in western Siberia: Effect of the micro-landscape, latitude position and permafrost coverage, Appl. Geochemistry, 53, 53–70, doi:10.1016/j.apgeochem.2014.12.004, 2015.

Stern, G. A., Macdonald, R. W., Outridge, P. M., Wilson, S., Chételat, J., Cole, A., Hintelmann, H., Loseto, L. L., Steffen, A., Wang, F., and Zdanowicz, C.: How does climate change influence arctic mercury?, Sci. Total Environ., 414, 22–42, doi:10.1016/j.scitotenv.2011.10.039, 2012.

Talbot, J., Moore, T. R., Wang, M., Ouellet Dallaire, C., and Riley, J. L.: Distribution of lead and mercury in Ontario peatlands, Environ. Pollut., 231, 890–898, doi:10.1016/j.envpol.2017.08.095, 2017.

Tamocai, C., Canadell, J. G., Schuur, E. A. G., Kuhry, P., Mazhitova, G., and Zimov, S.: Soil organic carbon pools in the northern circumpolar permafrost region, Global Biogeochem. Cycles, 23(2), 1–11, doi:10.1029/2008GB003327, 2009.

Trofimova, I. E., and Balybina, A. S.: Classification of climates and climatic regionalization of the West-Siberian plain, Geogr. Nat. Resour., 35(2), 114–122, doi:10.1134/S1875372814020024, 2014.

Velichko, A. A., Timireva, S. N., Kremenetski, K. V., MacDonald, G. M., and Smith, L. C.: West Siberian Plain as a late glacial desert, Quat. Int., 237(1–2), 45–53, doi:10.1016/j.quaint.2011.01.013, 2011.

Vishnyakova, E.K., and Mironycheva-Tokareva, N.P.: Moss decomposition in Western Siberian mires, in: Mosses: Ecology, Life Cycle and Significance, edited by: Pokrovsky, O., Volkova, I., Kosykh, N., and Shevchenko, V., 4th ed. Nova Science Publishers Inc. New York, pp. 217–241. 2018

Vorobyev, S. N., Pokrovsky, O. S., Serikova, S., Manasypov, R. M., Krickov, I. V., Shirokova, L. S., Lim, A., Kolesnichenko, L. G., Kirpotin, S. N., and Karlsson, J.: Permafrost boundary shift in Western Siberia may not modify dissolved nutrient concentrations in rivers, Water (Switzerland), 9(12), doi:10.3390/w9120985, 2017.

Wang, X., Yuan, W., Lin, C.-J., Zhang, L., Zhang, H., and Feng, X.: Climate and Vegetation As Primary Drivers for Global Mercury Storage in Surface Soil, Environ. Sci. Technol., 53(18), 10665–10675, doi:10.1021/acs.est.9b02386, 2019.

https://doi.org/10.5194/bg-2019-483
Preprint. Discussion started: 28 January 2020

Wilhelm, R. C., Niederberger, T. D., Greer, C., and Whyte, L. G.: Microbial diversity of active layer and permafrost in an acidic wetland from the Canadian high arctic, Can. J. Microbiol., 57(4), 303–315, doi:10.1139/w11-004, 2011.

Zhang, Y., Jacob, D. J., Dutkiewicz, S., Amos, H. M., Long, M. S., and Sunderland, E. M.: Biogeochemical drivers of the fate of riverine mercury discharged to the global and Arctic oceans, Global Biogeochem. Cycles, 29(6), 854–864, doi:10.1002/2015GB005124, 2015.

https://doi.org/10.5194/bg-2019-483
Preprint. Discussion started: 28 January 2020

Biogeosciences Discussions

Table 1. Mean (± SD) concentrations and stocks of C and Hg in 6 studied sites of WSL peatbogs.

Horizons	**C, %**	**Hg, ng g^{-1}**	**kg C m^{-2}**	**mg Hg m^{-2}**	**R_{HgC} (μg g^{-1})**
Plotnikovo (Pl), Southern taiga, 56.9°N*					
ALT (0-140 cm)	45±2	36±12	24	2.8	0.08±0.03
Mineral (140-150 cm)	13	53	23	9.0	0.40
Total (150 cm)	43±8	37±12	47	11.8	0.10±0.09
0-30 cm	44±2	44±5	3	0.3	0.10±0.01
0-100 cm	45±2	36±10	9	0.8	0.08±0.02
Mukhrino (Mh), Middle taiga, 60.9°N*					
ALT (0-360 cm)	53±7	26±13	67	4.3	0.05±0.03
Mineral (360-380 cm)	15±19	24±19	51	8.3	0.46±0.46
Total (380 cm)	51±10	26±19	118	12.6	0.07±0.12
0-30 cm	50±0.4	29±7	4	0.3	0.06±0.02
0-100 cm	52±5	32±17	18	1.3	0.06±0.04
Kogalym (Kg), Northern taiga, 62.3°N*					
ALT (0-175 cm)	48±4	48±30	93	8.7	0.10±0.06
Mineral (175-190 cm)	10±13	12±10	17	2.3	0.34±0.36
Total (190 cm)	45±12	45±30	110	11	0.12±0.12
0-30 cm	45±1	65±19	3	0.5	0.14±0.04
0-100 cm	47±2	49±34	38	3	0.11±0.07
Khanymey (Kh), Northern taiga, 63.8°N					
ALT (0-34 cm)	44±2	64±43	17	2.1	0.15±0.10
PF1 (34-100 cm)	50±2	47±13	78	7.6	0.09±0.02
PF2 (34-138 cm)	48±6	47±11	119	11.8	0.10±0.02
Mineral (138-147 cm)	1±1	4±1	2	0.5	0.31±0.13
Total (147 cm)	42±16	47±28	138	14.4	0.13±0.09
0-30 cm	43±1	71±46	13	1.8	0.17±0.11
0-100 cm	47±4	54±29	95	9.6	0.12±0.07
Pangody (Pg), Forest tundra, 65.9°N					
ALT (0-40 cm)	50±4	78±25	38	5.3	0.16±0.07
PF1 (40-100 cm)	53±4	61 ±25	54	6.6	0.11±0.04
PF2 (40-155 cm)	48±10	67±23	78	11.0	0.15±0.07
Mineral (155-185 cm)	3±1	24±11	15	12.5	0.88±0.28
Total (185 cm)	41±19	62±28	130	28.8	0.27±0.30
0-30 cm	50±5	83±26	26	4.0	0.17±0.07
0-100 cm	52±4	68±25	92	11.9	0.13±0.06
Tazovsky (Tz), Southern tundra, 67.4°N					
ALT (0-40 cm)	49±3	186±110	22	7.4	0.38±0.20
PF1 (40-100 cm)	46±3	109±28	27	6.3	0.23±0.06
PF2 (40-380 cm)	47±4	104±39	156	35.0	0.22±0.08
Mineral (380-405 cm)	14±5	152±65	60	64.7	1.24±0.66
Total (405 cm)	45±9	115±57	238	107.0	0.30±0.31
0-30 cm	49±4	209±120	16	6.0	0.42±0.21
0-100 cm	47±3	140±80	48	13.7	0.29±0.15

Footnote: ALT is Active Layer Thickness; PF1 is frozen peat, (ALT-100 cм); PF2 is frozen peat (ALT to mineral layer); 'Mineral' is mineral layer; 'Total' is total Hg content averaged over full sampled depth. *In permafrost-free zone, the ALT extends from the surface to the mineral layer.

https://doi.org/10.5194/bg-2019-483
Preprint. Discussion started: 28 January 2020

Biogeosciences Discussions
Open Access
EGU

Table 2. Estimated northern permafrost soil Hg inventory (Gg) for different depth ranges down to 300 cm. Hg pool uncertainties are reported as the interquartile range (IQR), i.e. the 25th to 75th percentiles of the Hg pool distribution estimates by a Monte Carlo method. Soil organic carbon (SOC) pools are from Hugelius et al. (2014).

depth range	soils	SOC	Hg Pool	IQR		Hg % of total per depth range
		Pg	Gg	Gg		
0-30 cm	organic (>20% SOC)	172	32	12	42	48
	mineral (<20% SOC)	45	35	16	45	52
	total	**217**	**67**	**37**	**88**	
0-100 cm	organic (>20% SOC)	253	47	24	61	21
	mineral (<20% SOC)	219	178	58	271	79
	total	**472**	**225**	**102**	**320**	
0-200 cm	organic (>20% SOC)	366	68	42	86	16
	mineral (<20% SOC)	461	364	192	493	84
	total	**827**	**433**	**257**	**564**	
0-300 cm	organic (>20% SOC)	427	79	52	99	14
	mineral (<20% SOC)	607	477	292	621	86
	total	**1035**	**557**	**371**	**699**	

Table 3. Comparison of estimated northern soil Hg pools by different studies.

			Schuster et al. 2018		Olson et al. 2018		this study	
depth range	SOC	95% CI	Hg Pool	95% CI	Hg Pool	25% CI	Hg Pool	IQR[1]
	Pg	Pg	Gg	Gg	Gg	Gg	Gg	Gg
0-30 cm	217	12	347	196	26	21-42[1]	67	37-88
0-100 cm	472	27	755	427	184	115-232[1]	225	102-320
0-200 cm	827	108	1323	764			433	257-564
0-300 cm	1035	150	1656	962			557	371-699

[1] Confidence interval (CI) corresponding to the 37.5th to 62.5th percentile

Table 4. Estimated Hg pool for different climate zones based on reported R_{HgC} and carbon pools. Hg pool uncertainties are reported as the interquartile range (IQR), i.e. the 25th to 75th percentiles of the Hg pool distribution estimates by a Monte Carlo method.

Climate zone	C pool	median RHgC	mean RHgC	Hg pool	fraction	IQR	
	Pg	(µg/g)	(µg/g)	Gg	(%)	Gg	
Tropics[1]	208	1.85	2.14	446	41.2	268	556
Subtropics[1]	102	1.83	2.13	217	20.0	128	271
Temperate[1]	191	1.35	1.55	297	27.4	186	367
Boreal[1]	140	0.36	0.42	57	5.2	38	69
Arctic[2]	217[3]	(0.15, 0.64)	(0.19, 0.77)	67	6.2	37	88
total	**858**			**1085**		**848**	**1258**

[1] Carbon pools are from FAO and ITPS (2018).
[2] The arctic R_{HgC} and Hg pool are from Table 2.
[3] The arctic carbon pool is from Hugelius et al. (2014)

https://doi.org/10.5194/bg-2019-483
Preprint. Discussion started: 28 January 2020

Biogeosciences
Discussions
Open Access

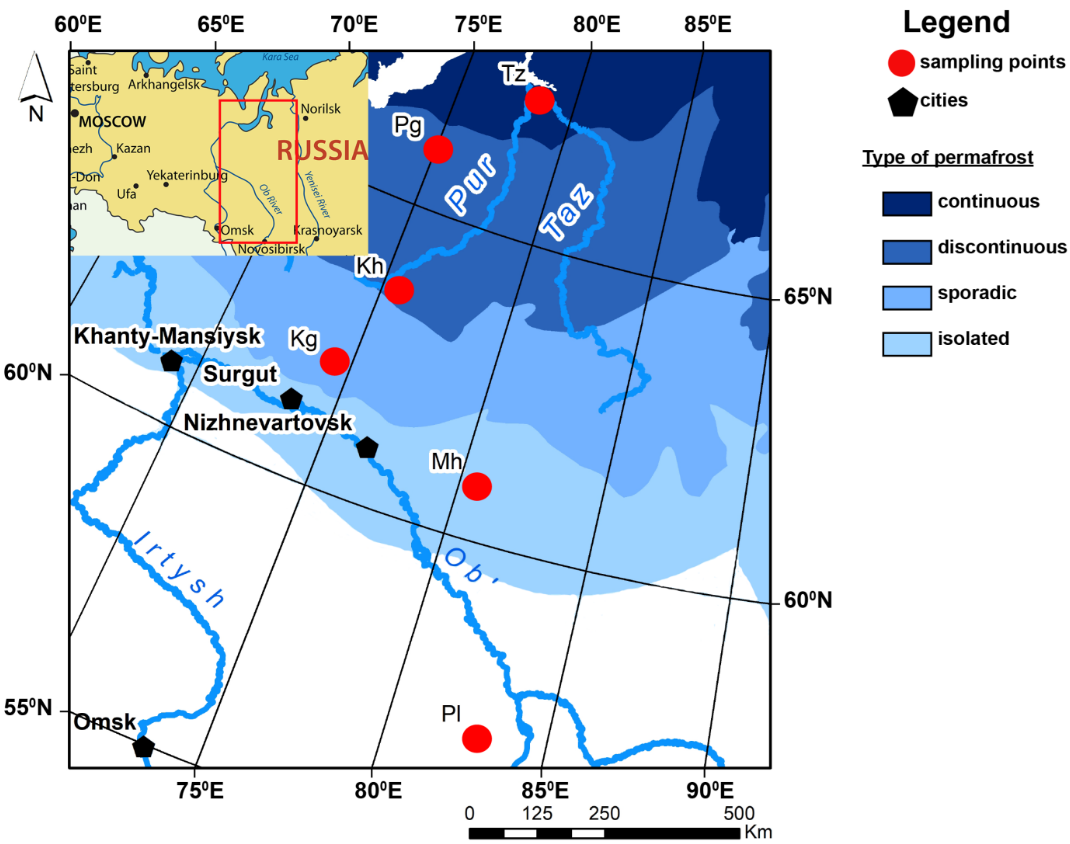

Fig. 1. Sampling sites and permafrost boundaries (modified after Brown et al., 2001) of WSL territory investigated in this work. The climate and soil parameters of 6 sampling sites (Tazovsky Tz, Pangody Pg, Khanymey Kh, Kogalym Kg, Mukhrino Mh, and Plotnikovo Pl) are listed in Supplementary Table S1.

https://doi.org/10.5194/bg-2019-483
Preprint. Discussion started: 28 January 2020

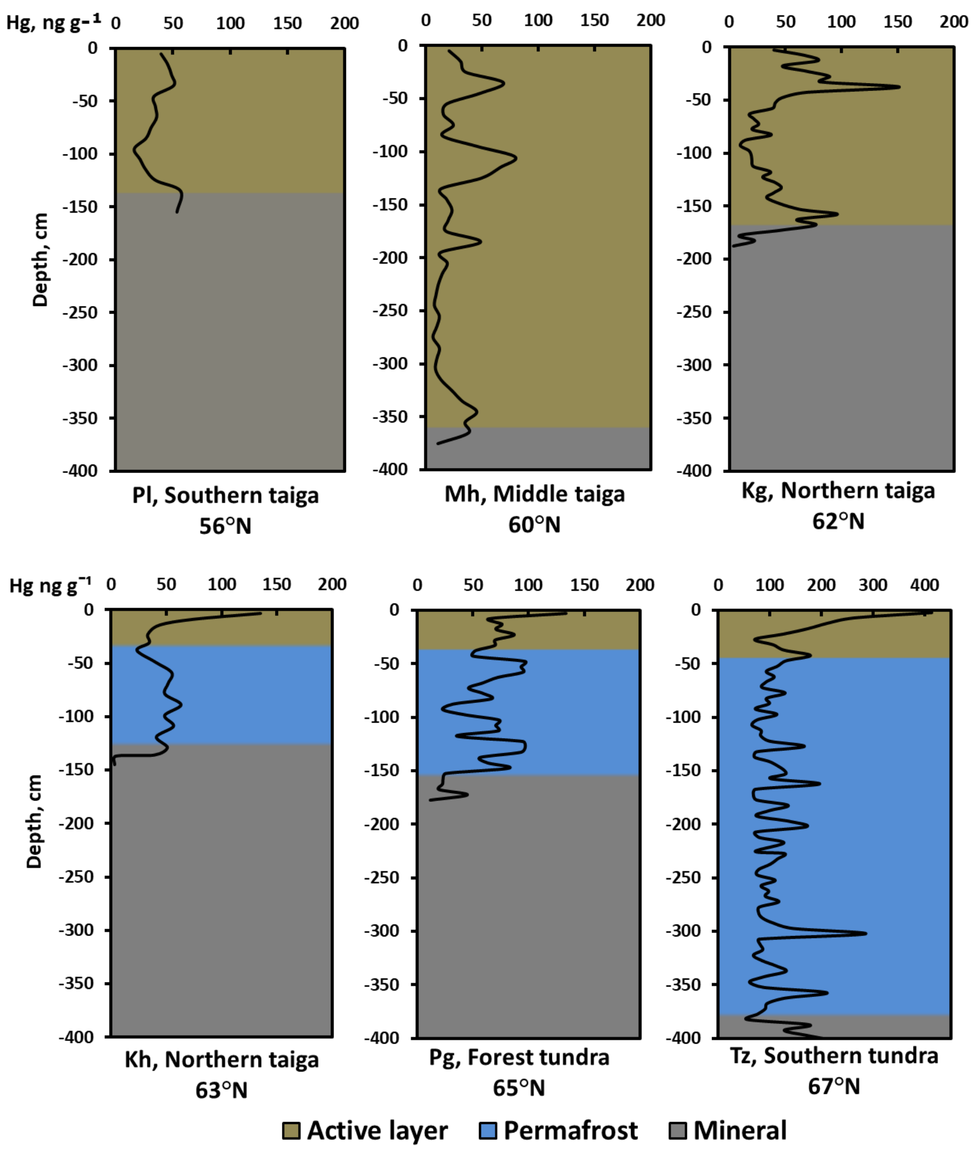

Fig. 2. Vertical depth profile distribution of total Hg (THg) in 6 peat cores across a 1700 km latitudinal transect of the WSL. Site location and physio-geographical parameters are shown in Fig. 1 and Supplementary Table S1.

https://doi.org/10.5194/bg-2019-483
Preprint. Discussion started: 28 January 2020

Biogeosciences
Discussions
Open Access
EGU

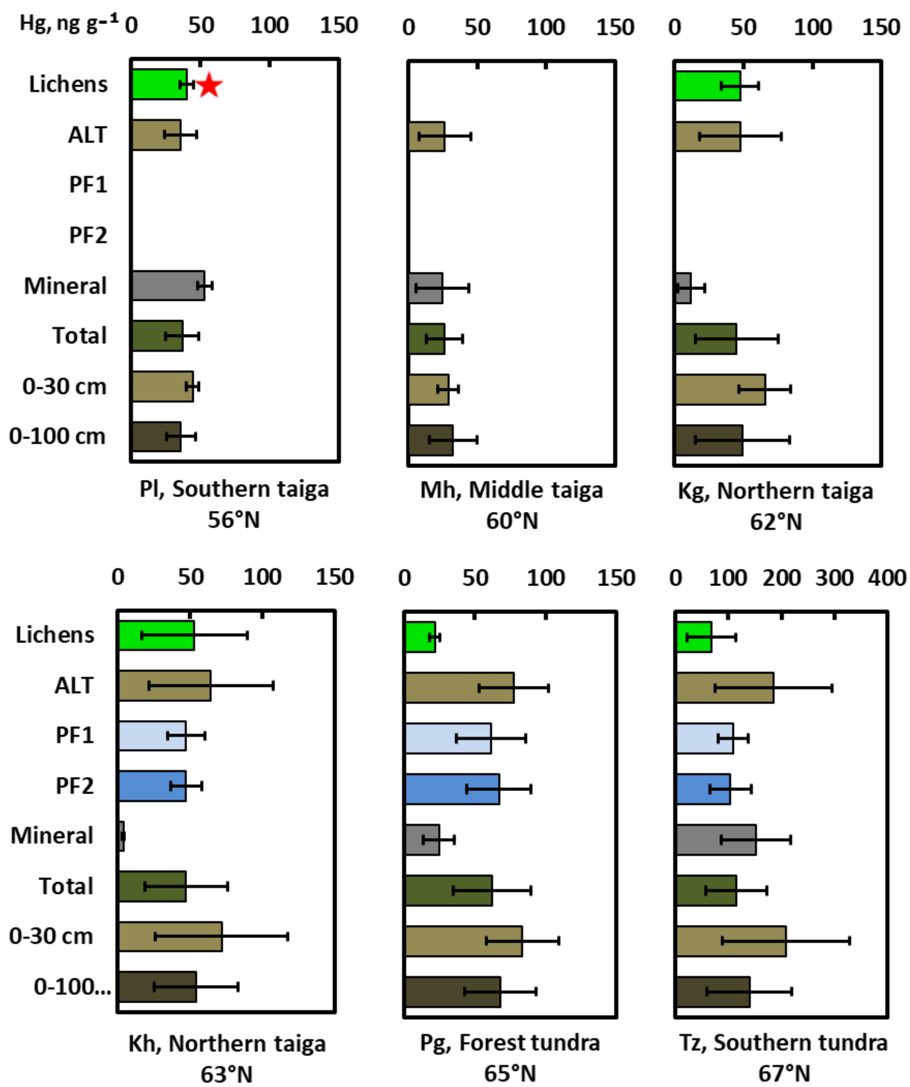

Fig. 3. Mean (±SD), depth-integrated Hg concentrations in peat columns and mineral layers of 6 studied sites. Red asterisk represents the data from Lyapina et al. (2009).

https://doi.org/10.5194/bg-2019-483
Preprint. Discussion started: 28 January 2020

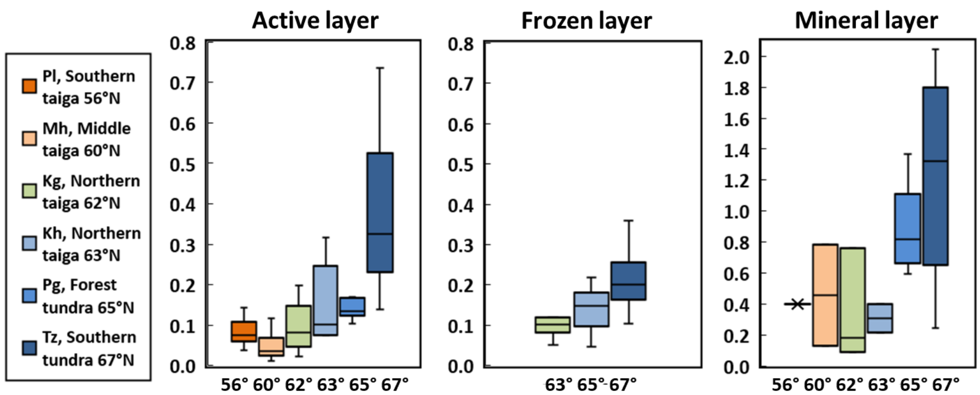

Fig. 4. The ratio Hg:C (µg:g), median±IQR, in the active layer, frozen peat and mineral horizons across the WSL latitudinal transect.

https://doi.org/10.5194/bg-2019-483
Preprint. Discussion started: 28 January 2020

Biogeosciences Discussions
Open Access

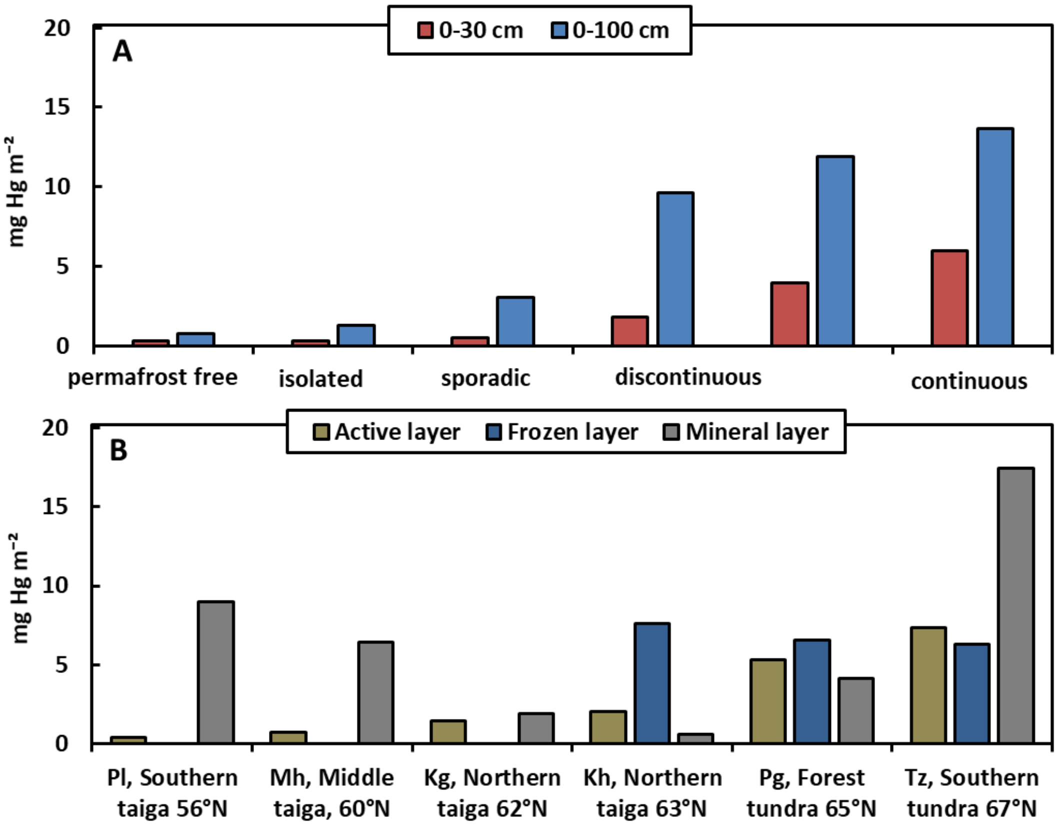

Fig. 5. Latitudinal variation in WSL soil Hg storage (mg Hg m^{-2}) in the 0-30 and 0-100 cm peat layer (**A**) and in the active, frozen and mineral layers (**B**). In the permafrost-free zone, the first 40 cm were used to calculate Hg storage in the active layer. The permafrost peat layer is fixed from the lower boundary of the active (unfrozen) layer down to 100 cm. Finally, for the mineral layer we considered only the first 10 cm below peat deposits across the full latitudinal gradient of the WSL peatland.

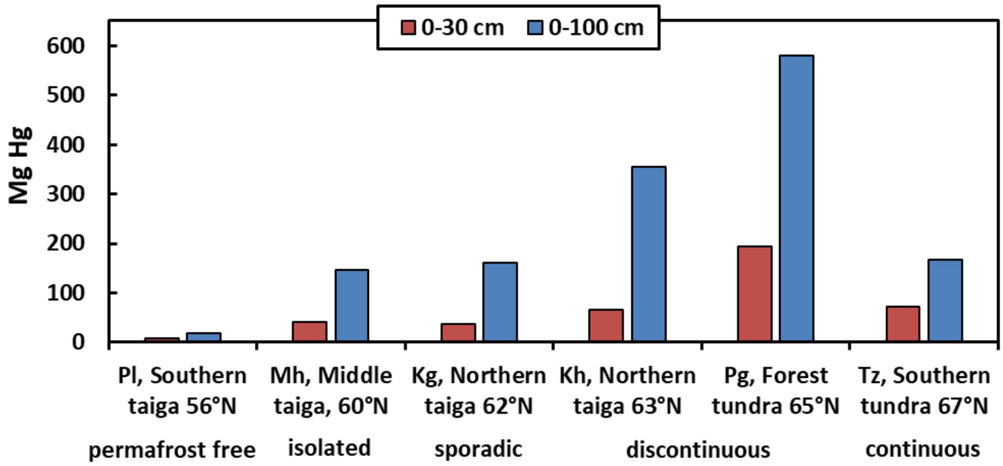

Fig. 6. Total, depth-integrated pools of Hg mass (Mg) in the upper 0-30 and 0-100 cm (red and blue columns, respectively) of WSL frozen peatlands in each permafrost zone. The stocks are calculated assuming the areal proportion of bogs from the landscape inventory across the WSL (Sheng et al., 2004).

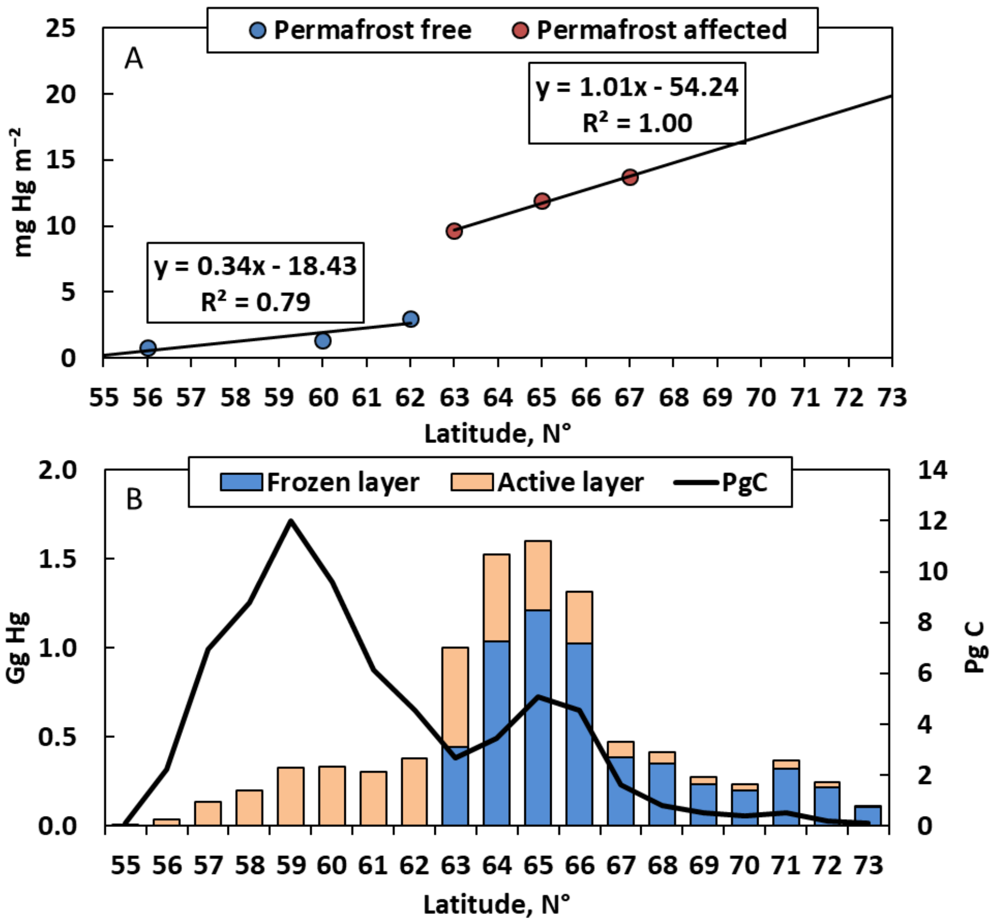

Fig. 7. Estimated Hg storage (mg Hg m^{-2}) in the 0-100 cm soil layer of the WSL (**A**) and latitudinal distribution of the Hg pool (Gg) in active and frozen peat layers of the WSL (**B**). Solid black line represents the WSL C pool (Pg) from Sheng et al. (2004).

Biogeosciences
Discussions
Open Access

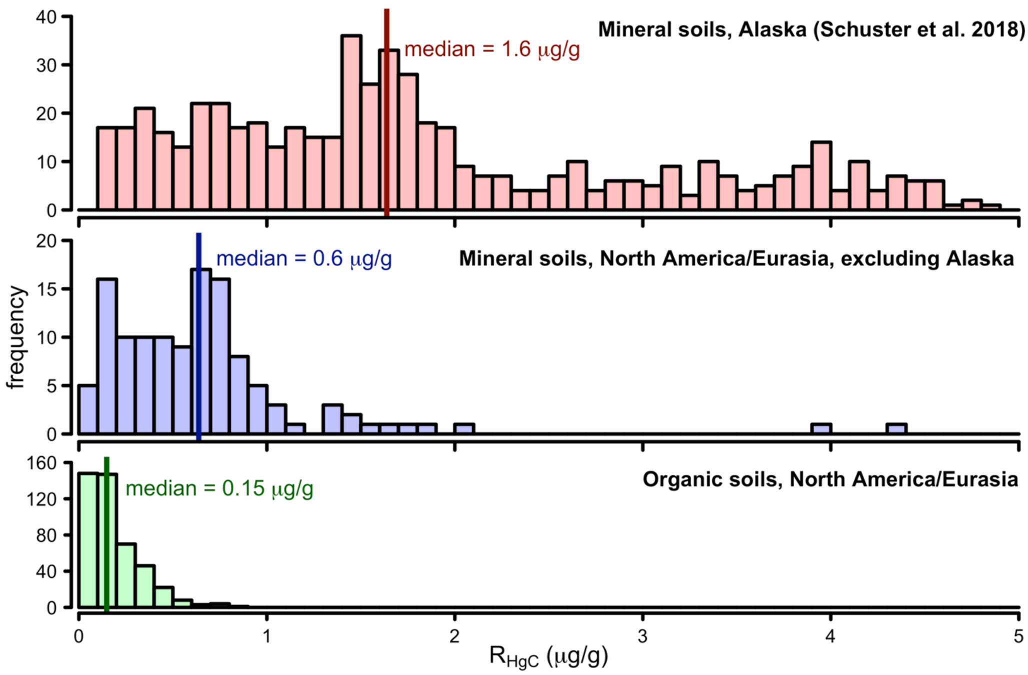

Fig. 8. Histogams of published and WSL R_{HgC} data used for estimating the northern soil Hg pool: Alaskan mineral soils (top, Schuster et al., 2018), mineral soils from North America, excluding Alaska, and Eurasia (middle), and organic soils from North America and Eurasia, including Alaska (lower).

https://doi.org/10.5194/bg-2019-483
Preprint. Discussion started: 28 January 2020

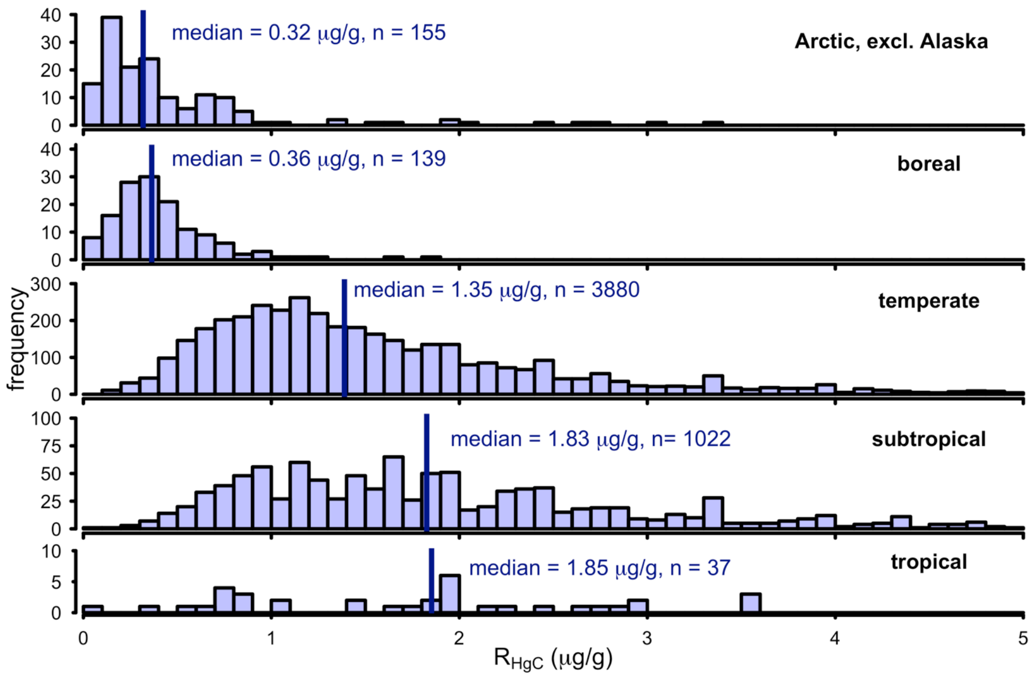

Fig. 9. Histograms and median R_{HgC} for different global climate zones.